CYCLIC OXIDATION OF FeCrAlY/Al_2O_3 COMPOSITES

James A. Nesbitt, Susan L. Draper, and Charles A. Barrett
NASA Glenn Research Center at Lewis Field
Cleveland, Ohio

Abstract

Three-ply FeCrAlY/Al_2O_3 composites and FeCrAlY matrix-only samples were cyclically oxidized at 1000° and 1100°C for up to 1000 1-hr cycles. Fiber ends were exposed at the ends of the composite samples. Following cyclic oxidation, cracks running parallel to and perpendicular to the fibers were observed on the large surface of the composite. In addition, there was evidence of increased scale damage and spallation around the exposed fiber ends, particularly around the middle ply fibers. This damage was more pronounced at the higher temperature. The exposed fiber ends showed cracking between fibers in the outer plies, occasionally with Fe and Cr-rich oxides growing out of the cracks. Large gaps developed at the fiber/matrix interface around many of the fibers, especially those in the outer plies. Oxygen penetrated many of these gaps resulting in significant oxide formation at the fiber/matrix interface far within the composite sample. Around several fibers, the matrix was also internally oxidized showing Al_2O_3 precipitates in a radial band around the fibers. The results show that these composites have poor cyclic oxidation resistance due to the CTE mismatch and inadequate fiber/matrix bond strength at temperatures of 1000°C and above.

Introduction

Metal matrix composites (MMC's) have received significant attention as potential compressor and turbine materials for aero gas turbine engines as a means to reduce weight and increase engine efficiency. These MMC's consist of high strength, low density fibers, such as SiC or Al_2O_3, embedded in a ductile matrix. The desired goal for the composite is high strength and toughness but at a lower density than conventional monolithic materials. To realize this goal, MMC's require a strong fiber/matrix bond in order to transfer the load from the matrix to the stronger fibers. FeCrAlY is a relatively ductile alloy with excellent high-temperature oxidation resistance.[1] Single-crystal Al_2O_3 fibers have both high strength and low density, and are stable in oxidizing environments. Hence, FeCrAlY/Al_2O_3 composites have been closely examined as a potential high-temperature composite material. Although the mechanical and thermophysical properties have been studied,[2,3] much less work has been performed to examine the high-temperature oxidation of this composite material. FeCrAlY/Al_2O_3 composites were tested for 1000 short thermal cycles (5 minutes/cycle) from room temperature to 727°C.[4] These test conditions showed no outward degradation or cracking of the composite. However, the short thermal cycle and moderate temperature did not emphasize oxidation. Hence, the purpose of the present study was to examine the cyclic oxidation behavior of these composites with a test to emphasize oxidative attack.

Experimental

FeCrAlY powder (nominal composition of Fe-24Cr-8Al-0.06Y at.%) was used as the starting material for the matrix. The fibers were c-axis oriented, single-crystal Al_2O_3 (sapphire) with nominal 125-140 μm diameter supplied by Saphikon, Inc. (Milford, NH). The FeCrAlY/Al_2O_3 composites and FeCrAlY matrix-only samples were fabricated using the powder cloth technique.[5] In this fabrication process, FeCrAlY powder is blended with a fugitive organic binder to produce a pliable "dough." This dough is rolled into flexible cloth-like sheets and cut to fit into a hot press die. An Al_2O_3 fiber mat is prepared by wrapping a continuous length of the fiber around a lathe-mounted drum. The fibers are coated with an organic binder to hold the fibers in place. The "fiber mat" is removed from the drum and also cut to the desired size and orientation to fit in the hot press die. The composite panel is assembled by stacking alternating layers of matrix cloth and fiber mat in the die. Molybdenum foil is used on the top and bottom of the composite stack to separate the composite material from the die pressing plates. The composite panel is heated at an intermediate temperature in the vacuum hot press to "burn off" the binders prior to application of higher temperatures and pressures. Three plies of fiber mat were used to produce a fiber volume fraction of approximately 25-30%. No porosity was apparent in the consolidated composites. Matrix-only samples were fabricated in an identical fashion without inclusion of the Al_2O_3 fiber mats.

After consolidation, individual samples were cut from the panel into approximately 1.2 x 2.4 x 0.066 cm samples. Samples were cut such that the fibers were aligned along the greater sample length. Hangar holes were machined through the matrix and fibers in one end of the sample (see Fig 2c for the typical sample geometry). The Mo foil, which had diffusion bonded to the panel surface, was removed by chemical etching. All surfaces were polished through 600 grit SiC paper and ultrasonically cleaned in acetone and ethanol. The end of one composite after polishing is shown in Fig 1. The FeCrAlY material was ferritic (BCC) with the presence of an occasional Fe/Cr yttride particle (Figs 1c,d). Energy dispersive spectroscopy (EDS) of the large polished surfaces of composite samples and matrix-only samples indicated some Mo contamination in certain regions of some samples. This Mo contamination produced a very obvious and distinct oxide on these samples which increased the weight change. The weight change for the Mo-contaminated samples is not reported except for a matrix-only sample discussed and shown below.

Samples were cyclically oxidized for 1000 cycles at 1000°C and 200 cycles at 1100°C. Each cycle consisted of 1 hour at temperature with a minimum cool of 20 minutes at ambient room temperature. Samples were periodically removed from the cyclic oxidation rig, weighed and examined before further testing. Details of the cyclic oxidation rigs are given elsewhere.[6] Surfaces were examined by scanning electron microscopy (SEM) and energy dispersive spectroscopy (EDS), and surface oxide phases were identified by x-ray diffraction (XRD). Some samples were also cross-sectioned perpendicular to the fibers, mounted and polished by standard metallographic techniques.

Results

Specific weight change after cyclic oxidation at 1000° and 1100°C is shown in Figs 2a,b. At both temperatures, the composite gained more weight than the matrix-only samples. At 1100°C, the matrix-only material exhibited parabolic-like behavior (i.e., weight gain proportional to time$^{1/2}$) typical of FeCrAlY materials with good Al_2O_3 scale adherence. At 1000°C, the matrix-only sample showed an almost linear increase in weight with time after 200 cycles. This behavior is believed due to the Mo contamination and non-protective oxide formation on the corner of this sample (Fig 2c). The nearly linearly weight gains for the composites labeled as "1" in Figs 2a,b can be rationalized as the consequence of extra oxide growth around the exposed fibers and in cracks which developed in the matrix (see below). However, the unusually rapid initial weight gain and the following parabolic-like behavior of composite "2" in Fig 2a is unexplained. XRD of the large sides of the composite and matrix-only samples showed only the presence of α-Al_2O_3 on the surface at both temperatures (except for the regions of obvious Mo contamination).

The same location on the end of the same composite sample after 50 and 100 cycles at 1000°C is shown in Fig 3. After 50 cycles, it is apparent that the protective Al_2O_3 scale had spalled around some of the exposed fibers (see black arrows in Fig 3a). After 100 cycles, the extent of this preferential spalling around the fibers had increased (Fig 3b). It is interesting that most of this spallation had occurred around fibers in the middle ply or on the inner half of the fibers in the outer plies. Only one small area of oxide spallation, not associated with the fibers, was apparent (4 O'clock in Figs 3a,b). The size of this spalled area had not noticeably increased between 50 to 100 cycles. After only 50 cycles, gaps at the fiber/matrix interface were apparent around the outer half of many fibers in the outer fiber plies. The gaps appeared to have increased slightly between 50 and 100 cycles. Lastly, a crack was apparent between the two outer-ply fibers shown in Figs 3c,d. Although from this perspective it is impossible to know whether this crack was only in the oxide scale or penetrated into the matrix, it was apparent with further testing that large cracks between fibers did indeed penetrate into the matrix.

The micrographs in Fig 4 again show the same fiber located in the middle ply after 50, 100 and 1000 cycles at 1000°C. A region of spalled oxide between the two fibers (11 O'clock) in Fig 4a had been recovered with an oxide film containing a large crack after 50 additional cycles (Fig 4b). Several large regions of "virgin" oxide in Fig 4a contained cracks after longer exposures (e.g., compare the oxide plates at 10 O'clock and 1 O'clock in a, b and c). After 200 and 1000 cycles at 1000°C, some cracks between fibers in the outer plies appeared to link up either around or by having propagated through a fiber (Fig 5). Fe and Cr-rich oxides were sometimes observed to be growing from some of these cracks (Fig 6). Examining the exposed fiber ends from an oblique angle showed that the thermal cycling had caused the matrix to extend beyond the end of many of the fibers, especially those in the middle fiber ply (Fig 7). Cracks, both parallel and perpendicular to the fibers, developed in the large surfaces of the composites (Fig 8).

These cracks were noticed after several hundred cycles. On rare occasion, an Fe and Cr-rich oxide nodule could be observed growing out of the crack.

After cyclic oxidation at 1100°C, protective scale damage around the exposed fiber ends was more pronounced (Fig 9). The scale damage was again more prominent around the middle ply and the extension of the matrix past the fiber ends was again apparent (Figs 9bc). A cross-sectional view of "virgin" oxide shows a structure with a fine-grained outer layer above larger columnar grains (Fig 9d), typical of α-Al_2O_3 scales on FeCrAlY.[7,8] Cracks also developed in the large composite surface exposing what appeared to be multiple oxide layers (Fig 10). Only Al and O were detected by EDS in the open cracks.

Cross-sections made at a quarter and at half the length of the oxidized composites (perpendicular to the fibers) showed oxidation deep within the composite sample. Gaps around the fibers were still present at these locations far from the exposed fiber ends. Significant oxide had formed on the matrix at these gaps (Fig 11). EDS of this oxide layer indicated primarily Al_2O_3. In addition, a circular band of internal oxidation was present around some of the fibers (Figs 11b,c). EDS of the fine oxide precipitates also indicated Al_2O_3. As expected, the matrix in this internally oxidized region was depleted of Al.

Discussion

A major concern for continuous-fiber MMC's intended for use at high-temperatures is the difference, or mismatch, between the CTE of the matrix and the reinforcing fiber. Typically, the high-strength fiber has a lower CTE than the matrix. During thermal cycling, this CTE mismatch can cause stresses at the fiber/matrix interface both parallel to and perpendicular to the fiber direction (i.e., the fiber axis). In the following simple arguments, the composite is considered to be in a state of zero stress at room temperature. Considering first a direction parallel to the fibers, on heating, the matrix attempts to expand more than the fibers. With a strong fiber/matrix bond, this attempted expansion of the matrix loads the fibers in tension while the matrix, constrained by the fibers, is loaded in compression resulting in a shear stress at the fiber/matrix interface. If the shear strength of the fiber/matrix bond is less than this thermally-produced shear stress, the fiber/matrix interface will shear and the matrix will expand more than the fiber. Ideally, on cooling, the matrix and fibers would contract back to their original positions. However, any shear or sliding at the interface, oxidation at the interface, or oxidation of the newly exposed cylindrical matrix wall (see below) could impede the contraction of the matrix resulting in a permanent matrix strain.

Likewise, in a direction perpendicular to the fibers, a CTE mismatch during heating will cause the matrix to attempt to expand away from the fibers. This action results in a tensile stress in the radial direction at the fiber/matrix interface. This tensile stress at the interface is complicated in a multi-ply composite due to overlapping stress fields for adjacent fibers, but should be a maximum in the outer direction in the outer fiber ply. If the fiber/matrix bond is insufficient, a gap can form at this interface. Again,

ideally, on cool down, the matrix should contract back around the fibers eliminating any gaps. However, any oxide formation within the gap at the elevated temperature could inhibit the matrix from fully contracting around the fibers.

The FeCrAlY matrix material used in this study has a CTE of approximately $14x10^{-6}/K$.[4] The Al_2O_3 fiber has a CTE of approximately $9x10^{-6}/K$.[3] These composites have a fiber/matrix debond strength at room temperature of 191 MPa, as measured by push out tests.[3] As stated earlier, similar FeCrAlY/Al_2O_3 composites were able to survive 1000 short (5 minute) cycles to 727°C without any evidence of composite deterioration.[4] Apparently for these test conditions, the fiber/matrix bond strength was sufficient to withstand the CTE mismatch stresses during repeated cycling to 727°C. However, in the present study, the gaps which were observed between fibers and the matrix, and the greater expansion of the matrix relative to the fibers observed at the end of the composite can be directly attributed to the CTE mismatch and an insufficient fiber/matrix bond. In comparison to the earlier study,[4] the current study employed both a higher temperature and an extended hold time (1 hour) in the oxidizing environment. The increase in temperature accentuates the problem of the CTE mismatch, decreases the bond strength[3] while increasing the oxidation rate. Obviously, the extended oxidation period results in more oxidation. However, the relative role of each of these factors in comparing the successful results of the previous study with the catastrophic results of the present study is not clear.

Fiber/matrix bond strength can be significantly affected by the composite fabrication technique. For NiAl/Al_2O_3 composites, the powder cloth fabrication process produced debond shear strengths of 40-100 MPa while a binderless process produced bond strengths of 280 MPa.[9] Cyclic oxidation of the composites with the weaker bond at 1000° and 1200°C (1 hour cycles) resulted in significant matrix expansion and oxidation at the fiber/matrix interface.[10] In contrast, cyclic oxidation at the same temperatures of NiAl/Al_2O_3 composites fabricated with a binderless process resulting in a stronger bond showed significantly less gap formation or oxidation at the fiber/matrix interface although extension of the matrix beyond the exposed fiber ends was evident.[11]

Cyclic oxidation of both the strong and weakly bonded NiAl/Al_2O_3 composites resulted in matrix crack formation perpendicular to the fibers.[10,11] Doychak, et al.,[10] suggested a possible explanation related to oxidation while the matrix is expanded beyond the exposed fiber ends. Oxidation of the exposed cylindrical matrix wall would impede the matrix from fully contracting upon cooling to a position planar with the fiber ends. This offset between the fiber and matrix causes the matrix to remain in a state of tension. Repeated thermal cycling with the associated matrix expansion and oxidation could result in a periodic increase the tensile stress in the matrix. This matrix stress could be relieved by plastic flow of the matrix or by crack formation perpendicular to the fibers. Hence, the matrix cracks aligned perpendicular to the fibers, as observed in the previous studies with NiAl/Al_2O_3,[10,11] and in the present study, are likely the result of this oxidation/mechanical interaction.

Lee, et al.,[12] also performed cyclic oxidation of a FeCrAl-based matrix material (alloy MA956) reinforced with continuous single-crystal Al_2O_3 fibers. As part of this study, a micromechanical finite element analysis was conducted to attempt to explain observed surface cracks running parallel to the fibers. The results of this analysis predicted a maximum strain on the sample surface perpendicular to and located halfway between adjacent fibers. Cracking caused by this strain would be perpendicular to the strain, producing cracks parallel to the fibers, as observed in their study.[12] The same thermomechanical loading could be the cause for the cracks parallel to the fibers observed in the present study.

Conclusions

Mismatch between the CTE of the fiber and matrix produced protective scale damage around exposed fiber ends. The thermal cycling, assisted by oxidation, resulted in cracks both parallel to and perpendicular to the fibers on the large composite surface. In addition, cracks formed between fibers in the outer plies at the end of the composite. The fiber/matrix bond strength was insufficient to prevent gaps from forming at the fiber/matrix interface. The gaps and cracks resulted in significant oxidation within the composite. Consequently, the FeCrAlY/Al_2O_3 composites examined in this study are unsuitable for use at temperatures of 1000°C and above.

References

1. F.H. Stott, F.A. Golightly and G.C. Wood, "The Influence of Thermal Cycling on the Oxidation Behavior of Fe-Cr-Al and Fe-Cr-Al-Y Alloys at 1200°C,", Corrosion Science 19, 889-906, (1979).

2. S.L. Draper, B.M.J. Aikin, and J.I. Eldridge, "Tensile Behavior of Al_2O_3/FeAl + B and Al_2O_3 /FeCrAlY Composites,", Metall.Mater. Trans., 26A, 2719-2731 (1995).

3. B.J.M. Aikin, D.W. Petrasek, and S.L. Draper, "Thermal Expansion Behavior of Continuous fiber Reinforced Iron Based Alloys," HiTemp Review 1993, NASA CP 19117, p. 53-1 to 53-11 (1993).

4. D.J. Gaydosh, S.L. Draper, J.I. Eldridge, and P. Tsui, "Development of Alumina Reinforced FeAl and FeCrAlY," HiTemp Review 1990, NASA CP 10051, pp 39-1 to 39-12, (1990).

5. J.W. Pickens, R.D. Noebe, G.K. Watson, P.K. Brindley, and S.L. Draper, "Fabrication of Intermetallic matrix Composites by the Powder Cloth Process," NASA TM 102060, (1989).

6. C.A. Barrett and C.E. Lowell, "High Temperature Cyclic Oxidation Furnace Testing at Lewis Research Center," JTEVA, 10, 273-278, (1982).

7. V.K. Tolpygo, "The Morphology of Thermally Grown α-Al_2O_3 Scales on Fe-Cr-Al Alloys," Ox. Met., 51, 449-477, (1999).

8. C. Mennicke, E. Schumann, M. Rühle, R.J. Hussey, G.I. Sproule, and M.J. Graham, "The Effect of Yttrium on the Growth Process and Microstructure of α-Al_2O_3 on FeCrAl," Ox. Met., 49, 455-466, (1998).

9. R.R. Bowman, in *Intermetallic Matrix Composites II,* D.B. Miracle, D.L. Anton, and J.A. Graves (eds.), Mater. Res. Soc. Symp. Proc. 273, Pittsburgh, PA, 145- (1992).

10. J. Doychak, J.A. Nesbitt, R.D. Noebe, and R.R. Bowman, "Oxidation of Al_2O_3 Continuous Fiber-reinforced/NiAl Composites," Ox. Metals, 38, 45-72, (1992).

11. J.A. Nesbitt, R.R. Bowman and S.L. Draper, "Cyclic Oxidation of Al_2O_3/FeCrAlY and Al_2O_3/NiAl Composites," HiTemp Review 1994, NASA CP 10146, pp 48-1 to 48-13, (1994).

12. K.N. Lee, V.K. Arya, G.R. Halford, and C.A. Barrett, "Kinetics of Cyclic Oxidation and Cracking and Finite Element Analysis of MA956 and Sapphire/MA956 Composite System,' Met. and Mat. Trans., 27A, 3279-3291, (1996).

List of Figures

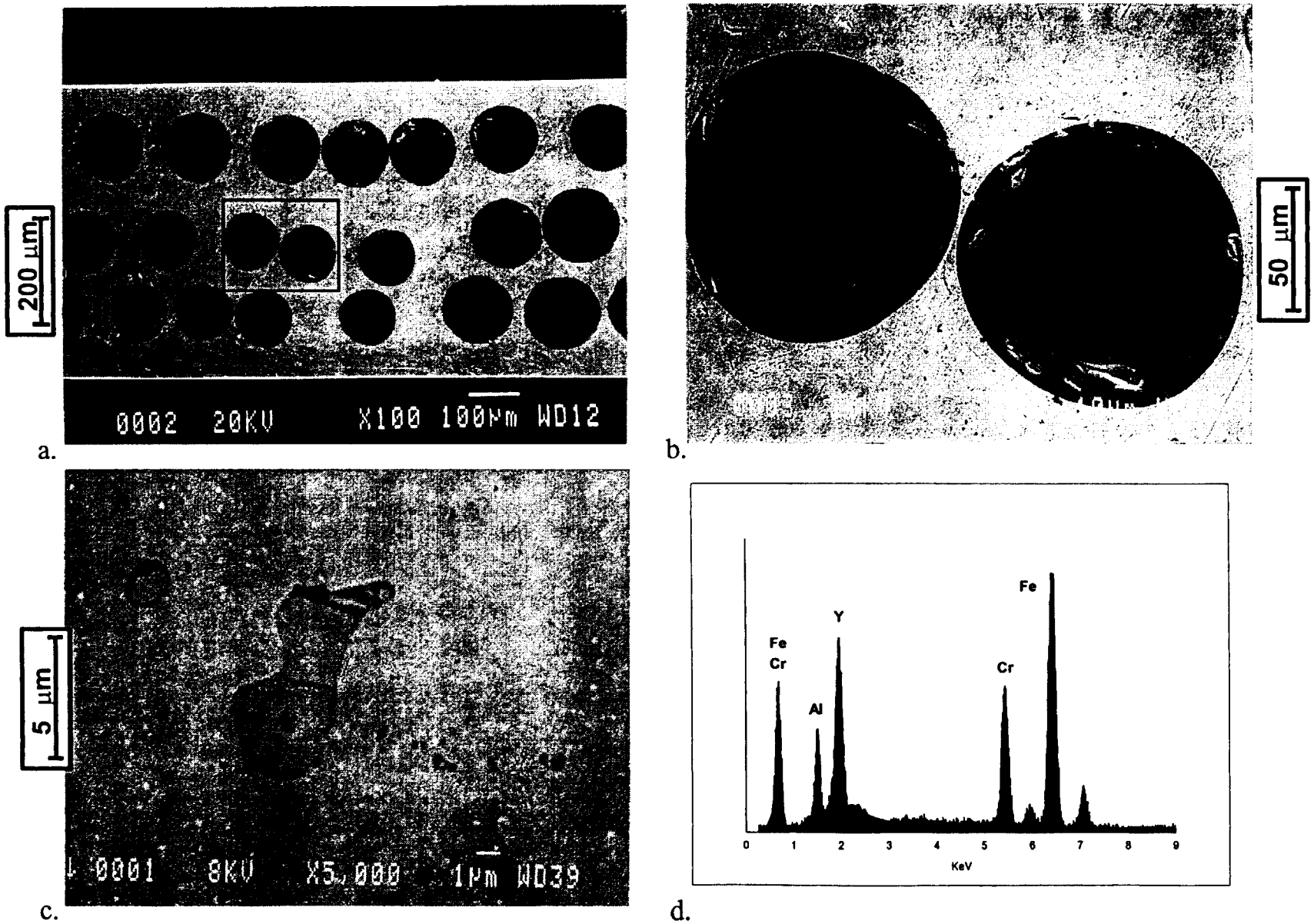

Fig 1 SEM micrographs of (a,b) the polished end of a composite sample showing the 3 plies and a magnified view of the fibers, (c) small Y-rich intermetallic particle in polished FeCrAlY matrix, and (d) EDS spectra of particle.

micron markers to be put on micrographs in final draft

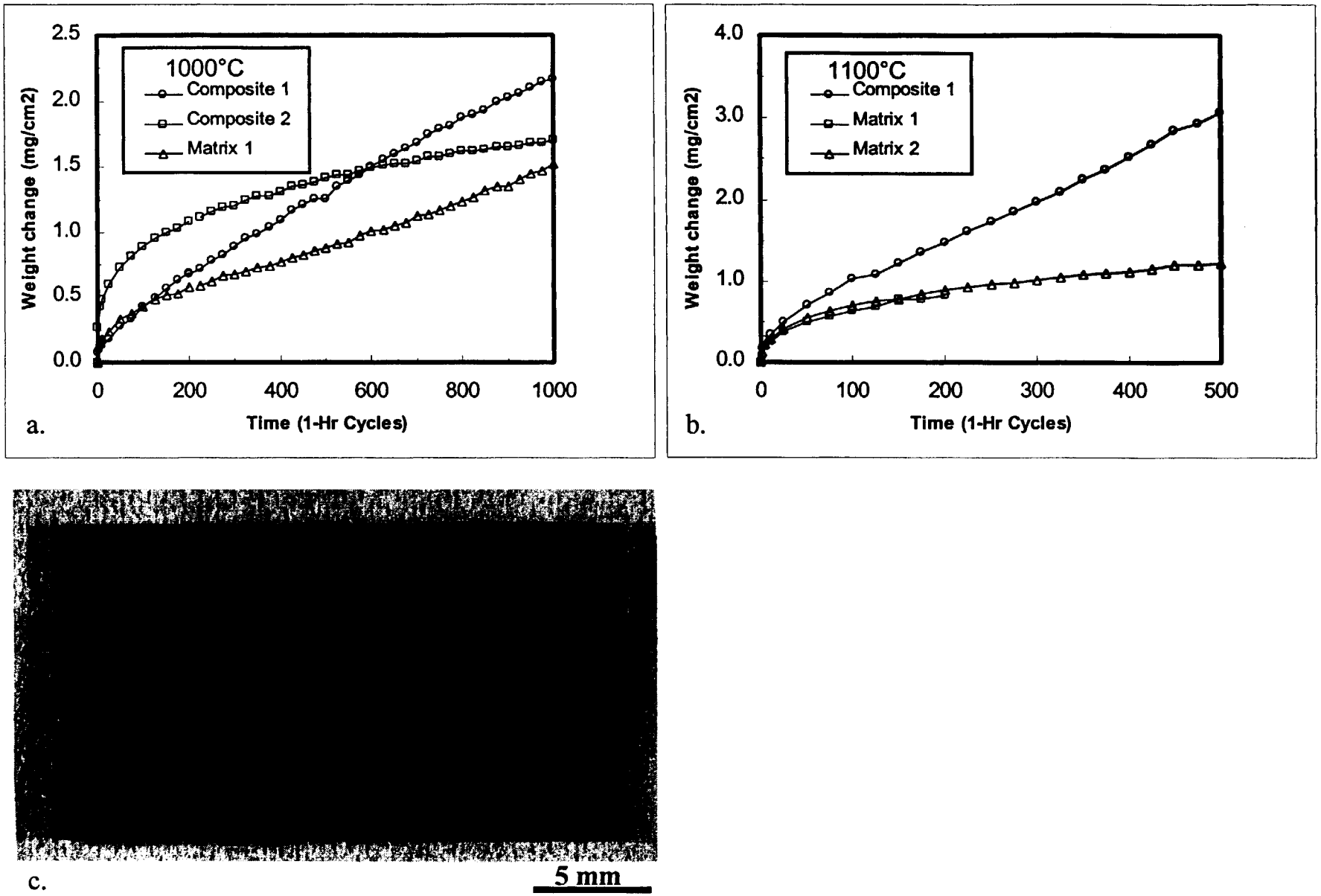

Fig 2 Specific weight change during cyclic oxidation at (a) 1000°C and (b) 1100°C. Mo-contamination in the upper right corner of the Matrix 1 sample tested at 1000°C is shown in (c).

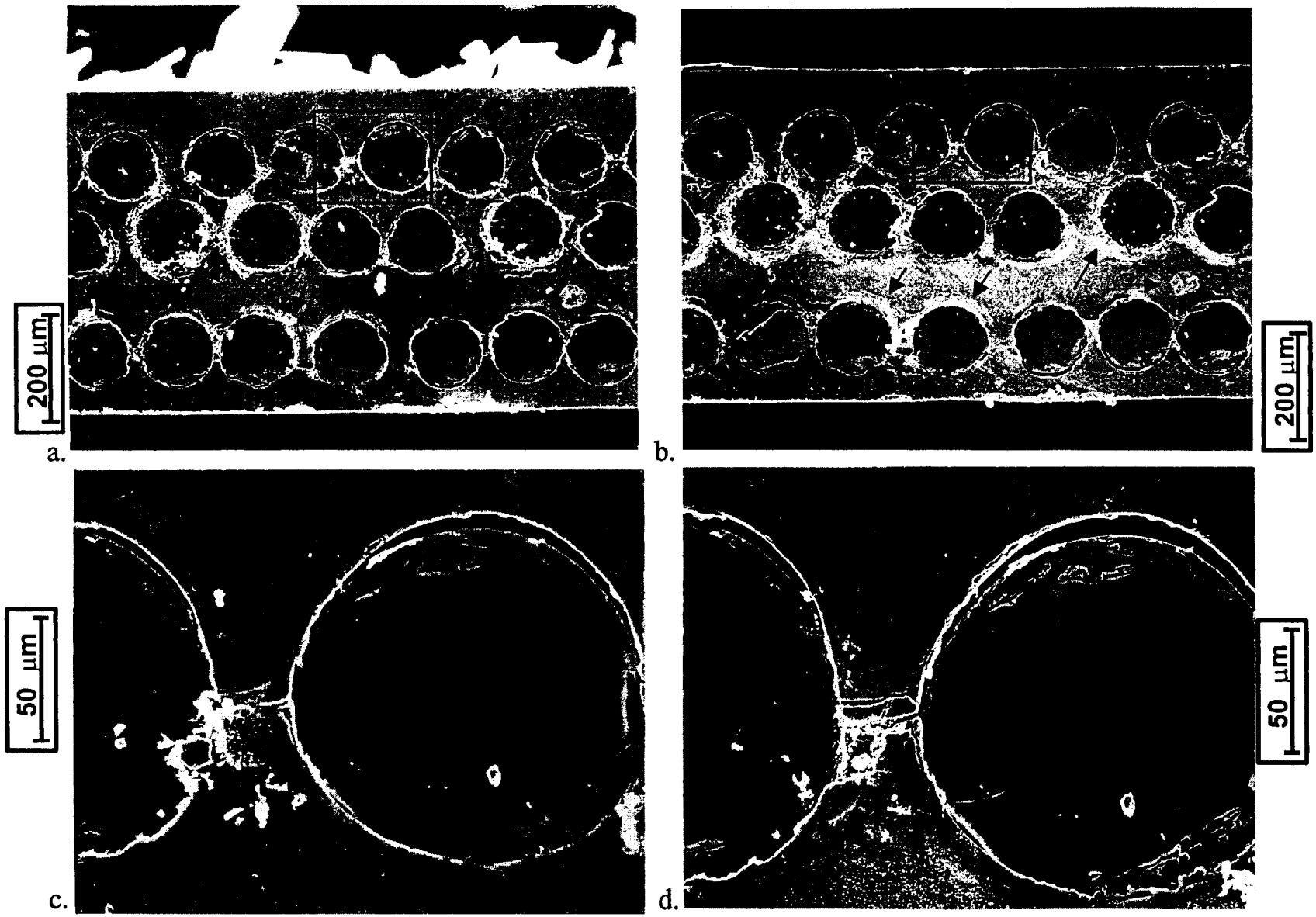

Fig 3 SEM micrographs of the same locations after (a,c) 50, and (b,d) 100 cycles. The location of the same two fibers in (c,d), after 50 and 100 cycles, are shown by the white rectangles in (a,b). Black arrows in (a,b) indicate areas of oxide spallation.

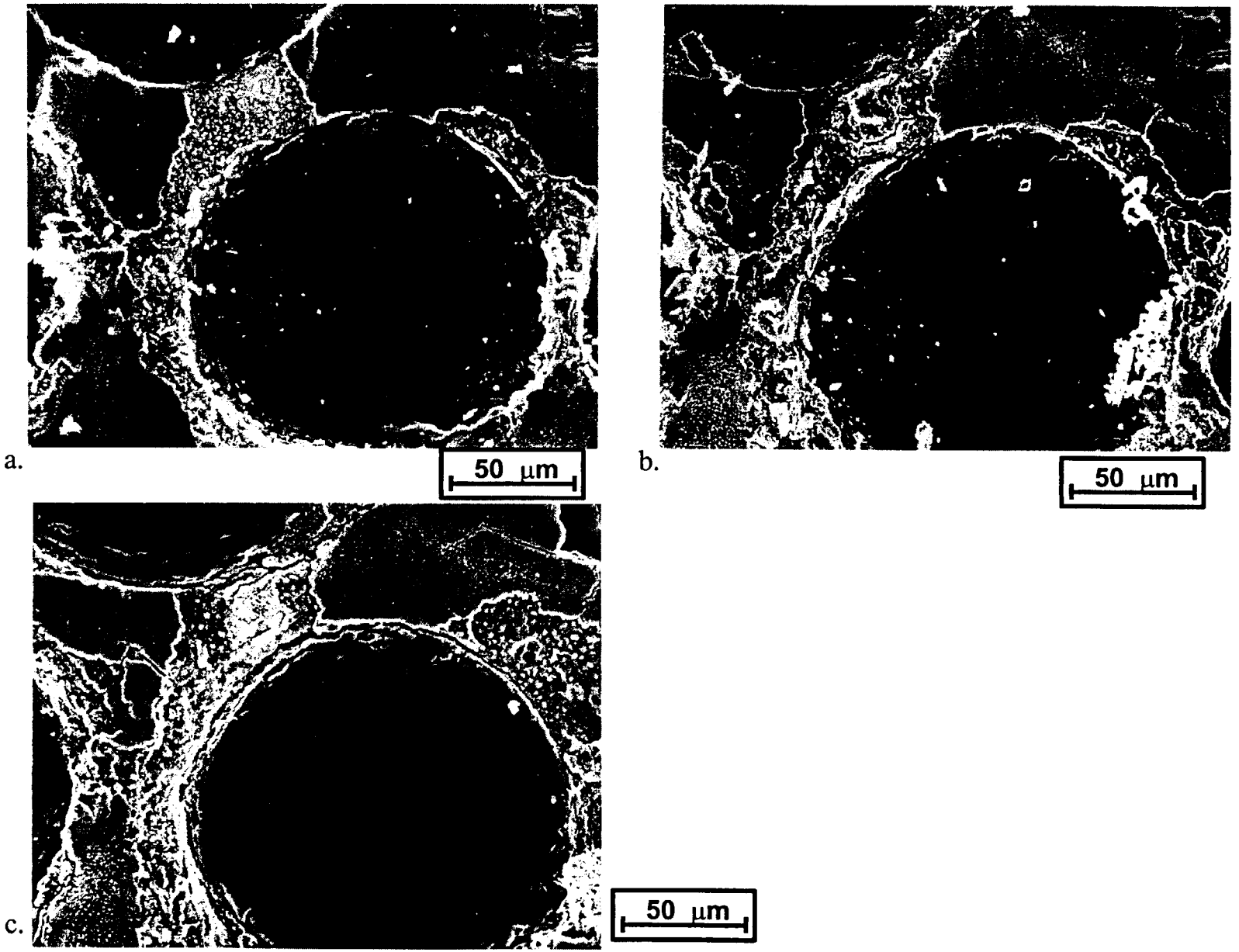

Fig 4 SEM micrographs of the same locations after (a) 50 cycles, (b) 100 cycles, and (c) 1000 cycles, 1000°C.

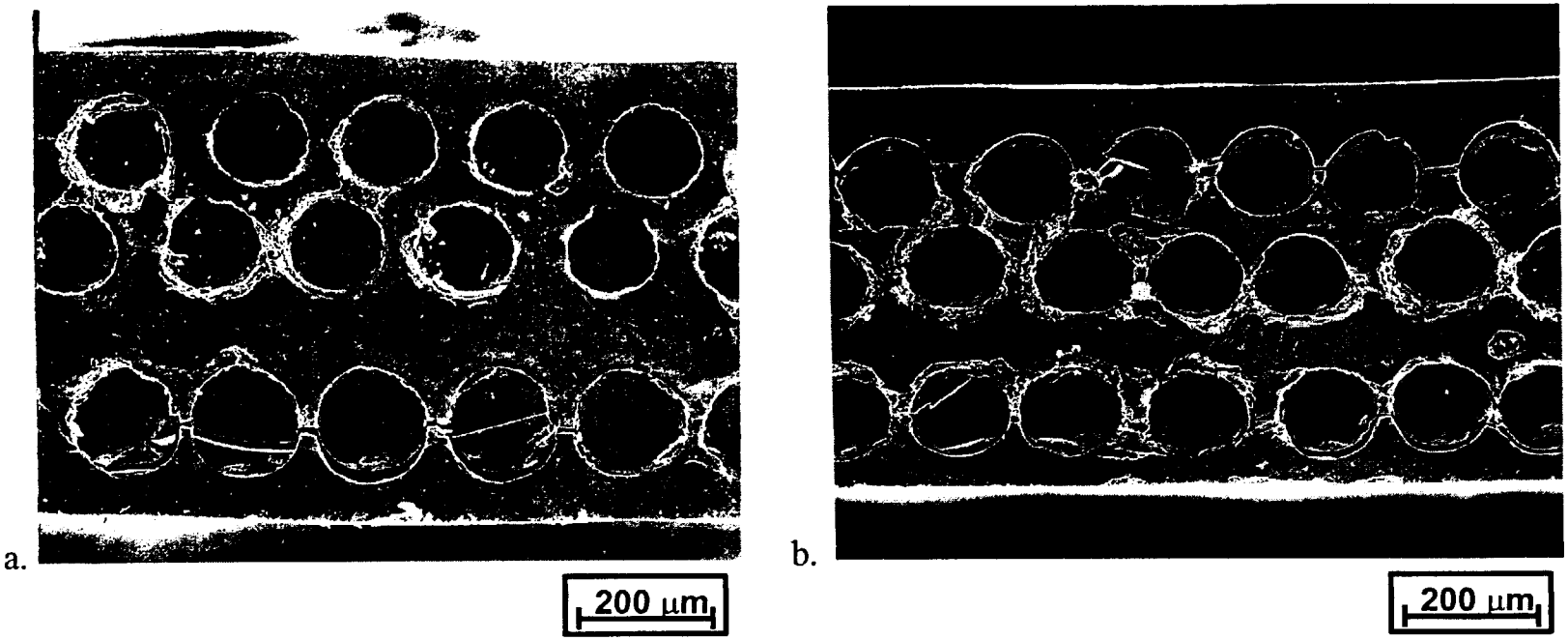

Fig 5 SEM micrographs of the composite after (a) 200 and , (b) 1000 1-hour cycles.

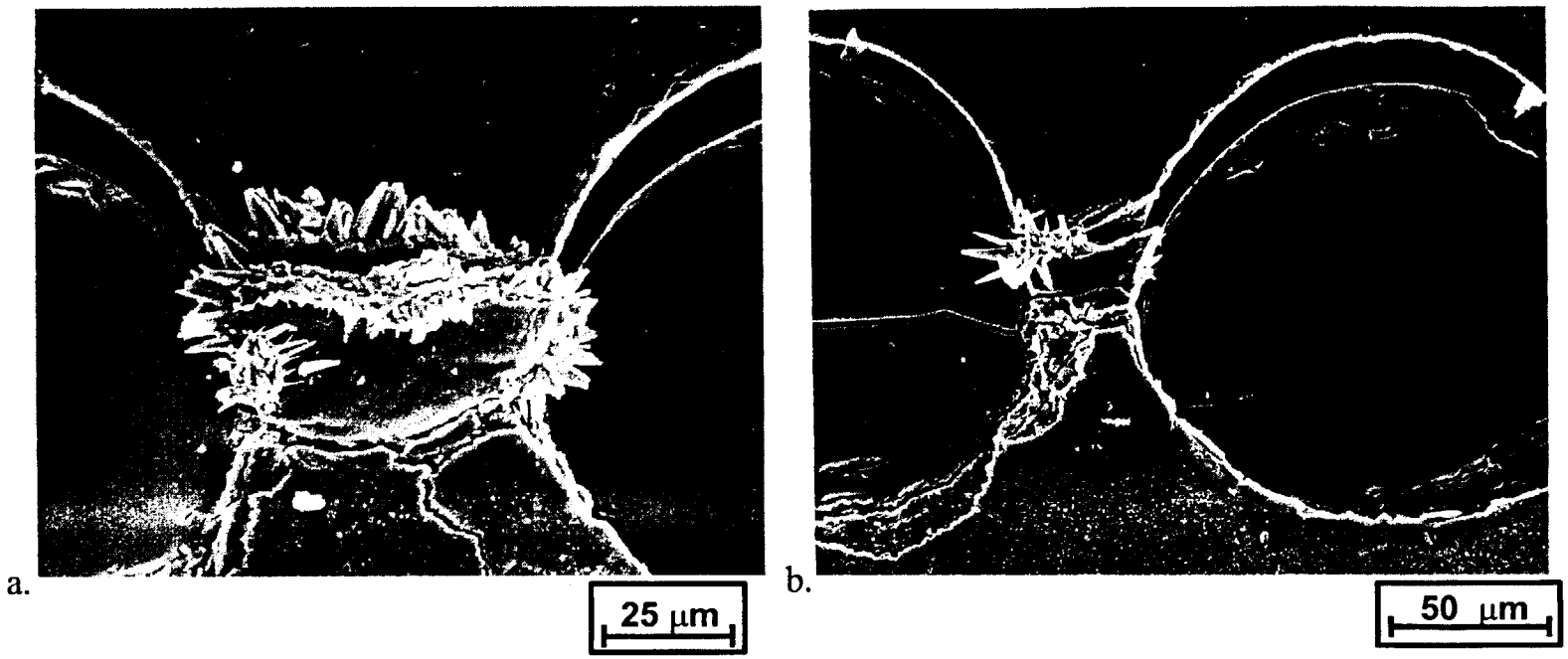

Fig 6 SEM micrograph of the end of the composite showing Fe and Cr-rich oxides growing at the cracks between fibers after 1000 1-hour cycles.

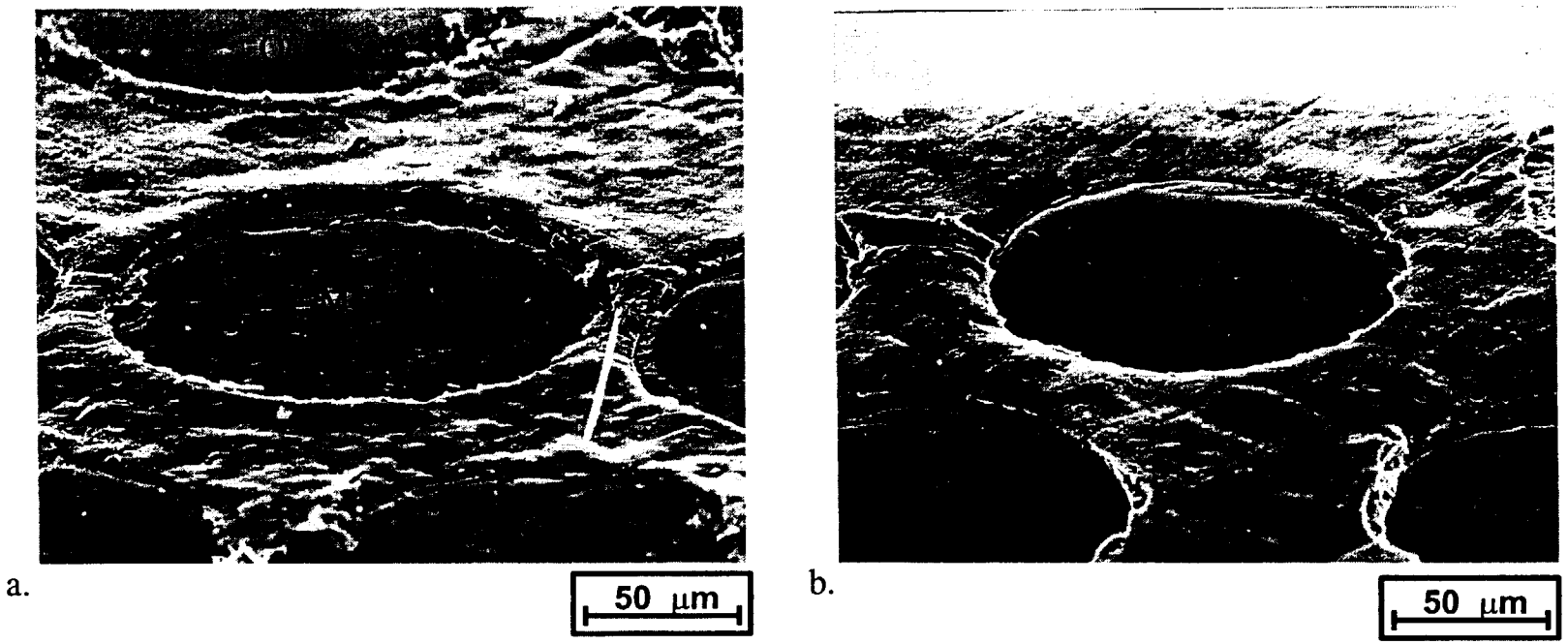

Fig 7 SEM micrographs of the composite after (a) 100 cycles (65° tilt), and (b) 1000 cycles (60° tilt). The letters M and O designate the middle and outer plies, respectively.

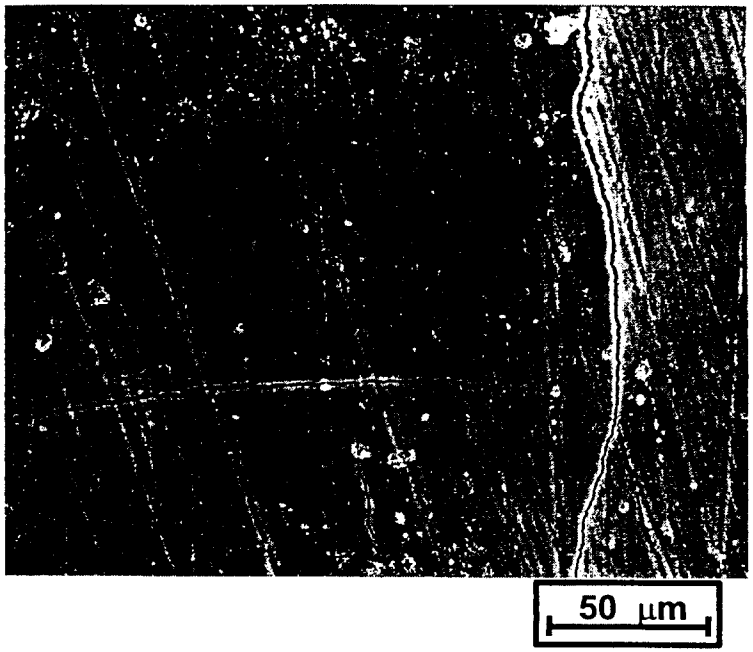

Fig 8 SEM micrographs showing cracks which developed in the large surface of a composite after 1000 cycles at 1000°C. Fiber direction is vertical.

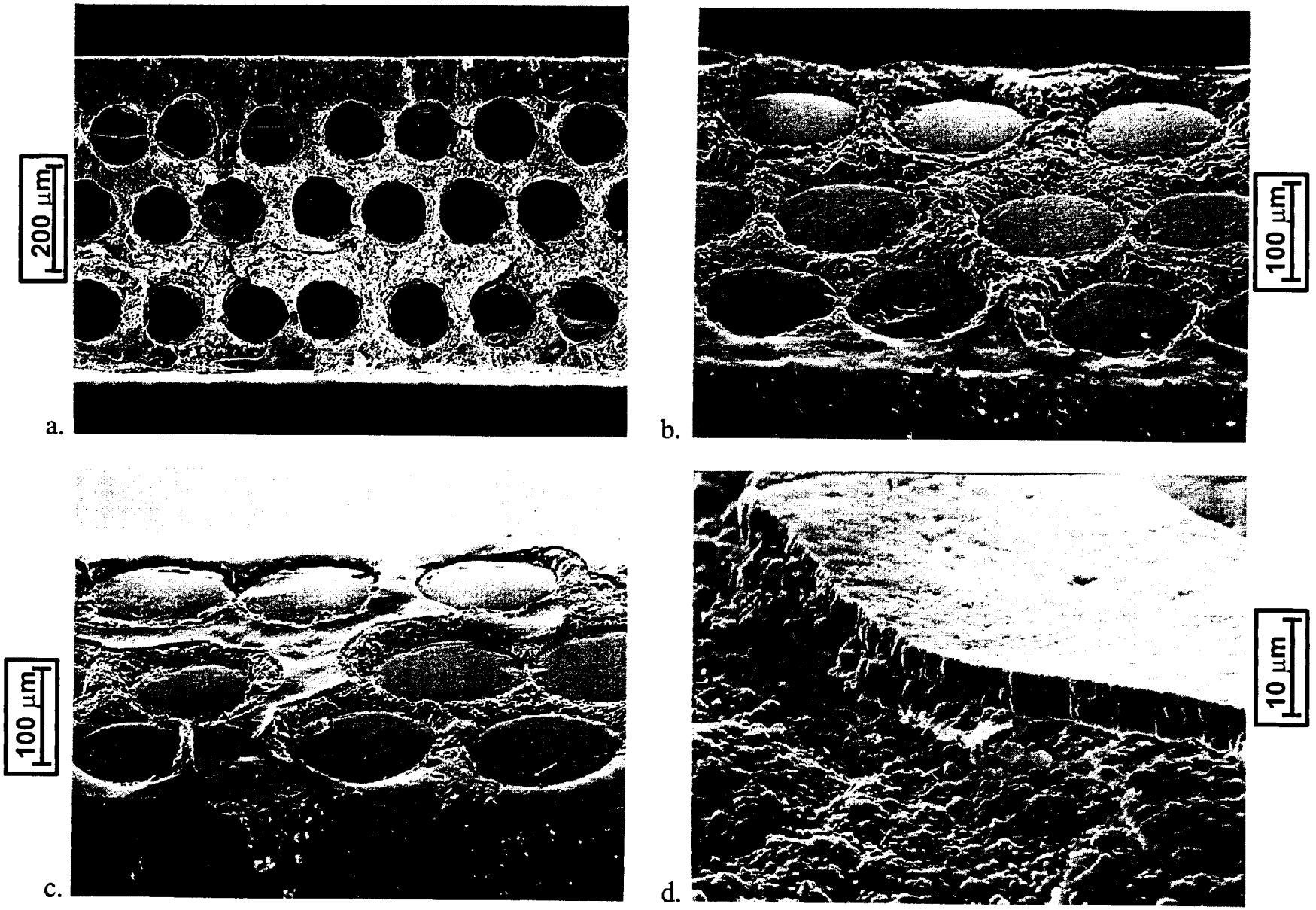

Fig 9 SEM micrographs of the ends of the composite after 100 cycles at 1100°C, (a), no tilt, (b,c,d) 65° tilt.

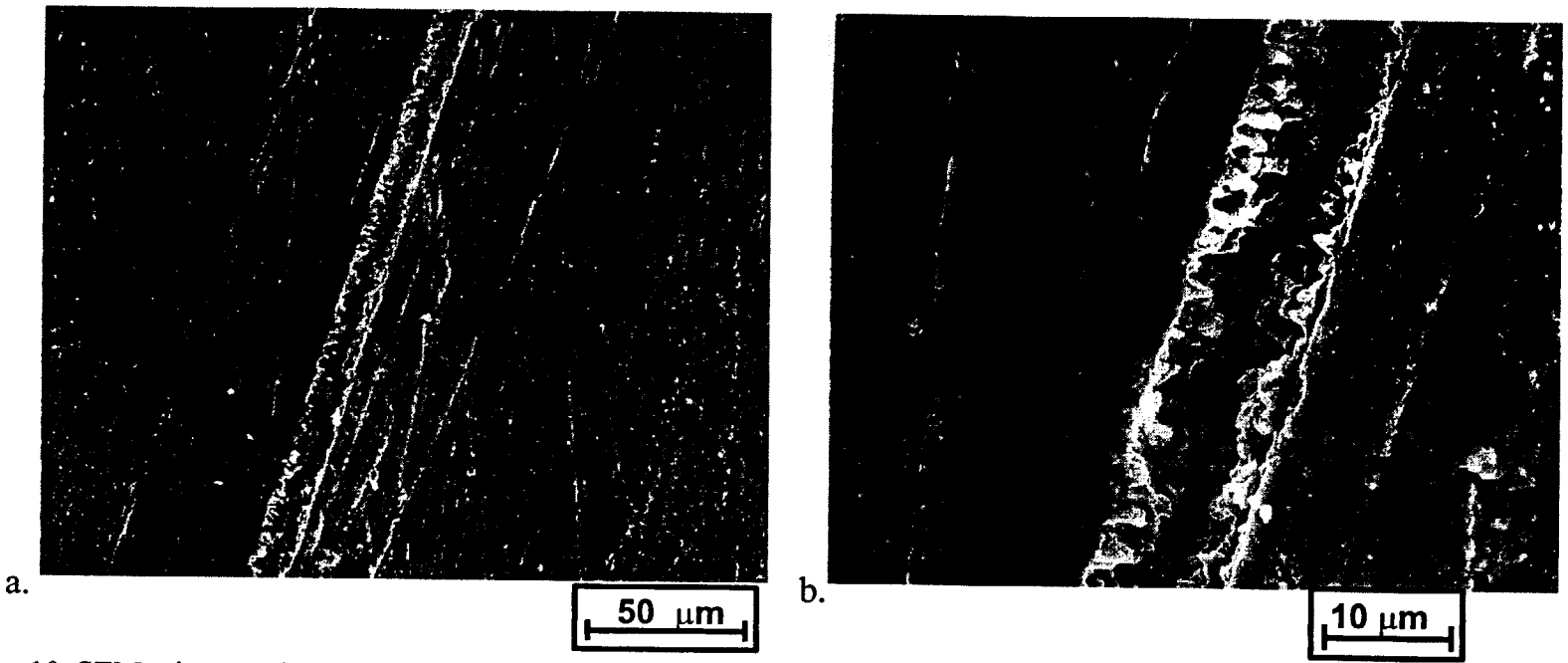

Fig 10 SEM micrographs of a crack in the surface of a composite after 200 cycles at 1100°C. (b) is a magnified view of (a). Fiber direction is vertical.

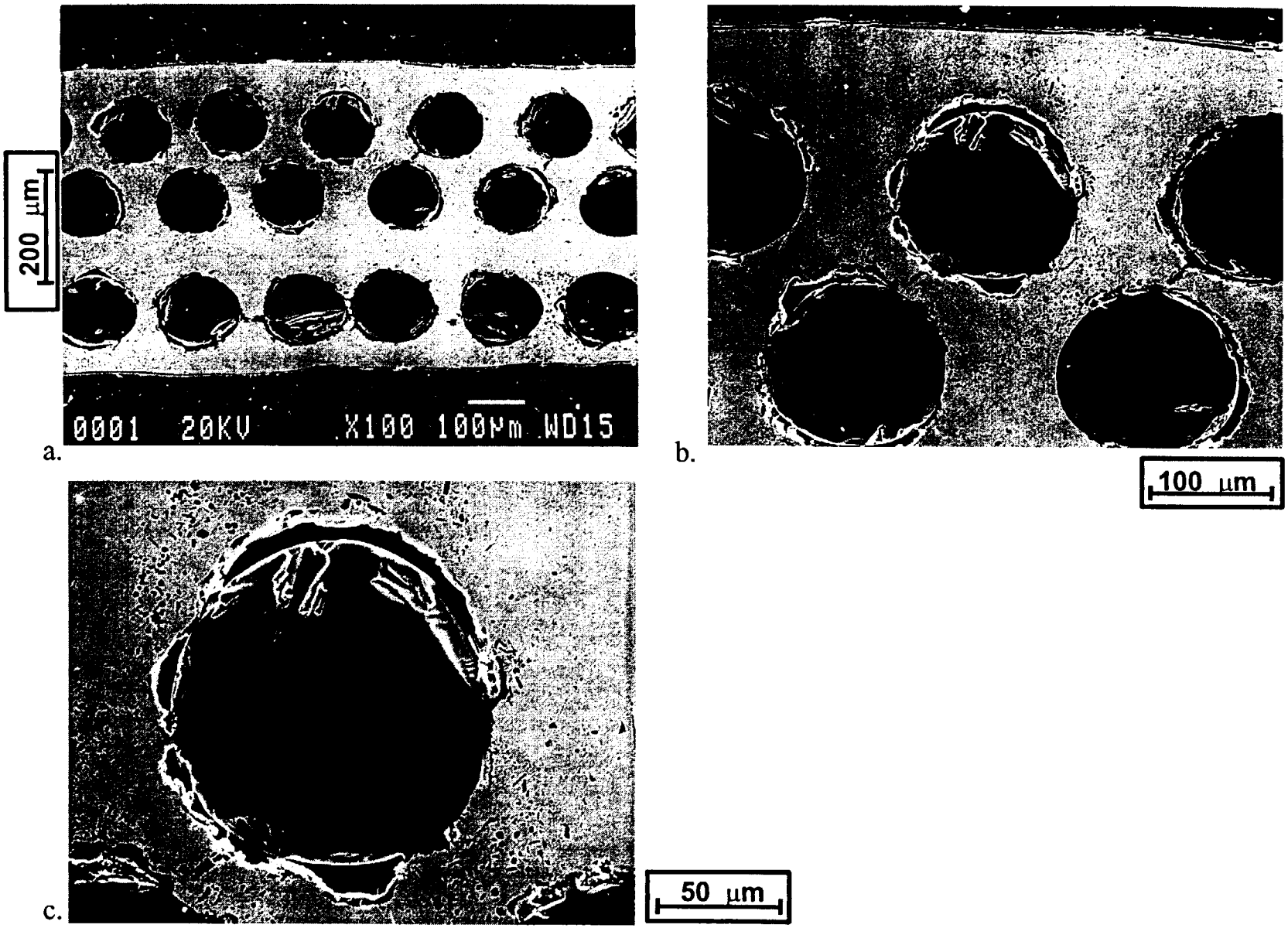

Fig 11 SEM micrographs of polished cross sections of the composite after 1000 1-hour cycles showing oxidation in the gaps between the fiber and matrix and internal oxidation of the matrix around one fiber. (b,c) are magnified views of (a).